Benzimidazoles as Metal-Free and Recyclable Hydrides for CO_2 Reduction to Formate

Chern-Hooi Lim[1,2*], Stefan Ilic[3,4], Abdulaziz Alherz[1], Brady T. Worrell[1], Samuel S. Bacon[1], James T. Hynes[2,5,6], Ksenija D. Glusac[3,4], and Charles B. Musgrave[1,2,7,8*]

[1]Department of Chemical and Biological Engineering, University of Colorado, Boulder, Colorado 80309, United States, [2]Department of Chemistry, University of Colorado, Boulder, Colorado 80309, United States, [3]Department of Chemistry, University of Illinois at Chicago, Chicago, IL 60607, United States. [4]Chemical Sciences and Engineering Division, Argonne National Laboratory, Lemont, IL 60439, United States, [5]PASTEUR, Département de Chimie, École Normale Supérieure, UPMC Univ. Paris 06, CNRS, PSL Research University, 75005 Paris, France, [6]Sorbonne Universités, UPMC Univ. Paris 06, École Normale Supérieure, CNRS, PASTEUR, 75005 Paris, France, [7]Materials Science and Engineering Program, University of Colorado, Boulder, Colorado 80309, United States, [8]National Renewable Energy Laboratory, Golden, Colorado 80401

KEYWORDS: CO_2 reduction, solar fuels, benzimidazole, organo-hydride, metal-free

ABSTRACT: We report a novel metal-free chemical reduction of CO_2 by a recyclable benzimidazole-based organo-hydride, whose choice was guided by quantum chemical calculations. Notably, benzimidazole-based hydride donors rival the hydride-donating abilities of noble metal-based hydrides such as $[Ru(tpy)(bpy)H]^+$ and $[Pt(depe)_2H]^+$. Chemical CO_2 reduction to the formate anion ($HCOO^-$) was carried out in the absence of biological enzymes, a sacrificial Lewis acid, or a base to activate the substrate or reductant. $^{13}CO_2$ experiments confirmed the formation of $H^{13}COO^-$ by CO_2 reduction with the formate product characterized by ^{1}H-NMR and ^{13}C-NMR spectroscopies, and ESI-MS. The highest formate yield of 66% was obtained in the presence of potassium tetrafluoroborate under mild conditions. The likely role of exogenous salt additives in this reaction is to stabilize and shift the equilibrium towards the ionic products. After CO_2 reduction, the benzimidazole-based hydride donor was quantitatively oxidized to its aromatic benzimidazolium cation, establishing its recyclability. In addition, we electrochemically reduced the benzimidazolium cation to its organo-hydride form in quantitative yield, demonstrating its potential for electrocatalytic CO_2 reduction. These results serve as a proof of concept for the electrocatalytic reduction of CO_2 by sustainable, recyclable and metal-free organo-hydrides.

INTRODUCTION

The chemical reduction of carbon dioxide (CO_2) to liquid fuels (e.g. methanol) powered by renewable energy would revolutionize the future energy landscape.[1-2] Such a technology could effectively close the carbon cycle; however, despite progress in the reduction of CO_2 to valuable products, no process has effectively met the requirements for the practical conversion of CO_2 to utilizable fuels. Furthermore, the scientific community has not yet reached a consensus on a general approach to address this challenge.

The reduction of CO_2 via hydride (H^-) transfer(s) stands as one of the most promising approaches to convert CO_2 to usable fuels,[3-5] with several reports describing progress towards implementation of such a system.[6-8] Of course, CO_2 cannot proceed directly to methanol by hydride transfers exclusively. An example is a recently proposed mechanism mediated by the organo-hydride dihydropyridine wherein CO_2 undergoes a series of three reductions, each one followed by a protonation: first, to generate formic acid (HCOOH), second, to produce methanediol — which converts to formaldehyde (CH_2O) with loss of water — and finally to generate methanol (CH_3OH).[9-10] This route may not always be effective, for example in cases where high activation barriers result in slow kinetics. A pteridine derivative is believed to undergo a similar pathway of CO_2 reduction, although the reduction by pteridines via this mechanism is not feasible due to slow kinetics.[11] In any event, the predicted mechanism of CO_2 reduction to methanol by hydride transfer we reported[9,10] was somewhat complex. While the individual steps involved were relatively simple, the overall route was complicated in two senses: first, multiple steps, hydride transfers, and proton transfers were involved; second, the preparation of the particular organic-hydride donor, dihydropyridine, involved electrode and photo-processes. This complexity suggests that an effective experimental scrutiny of the mechanism might focus on particular steps in the mechanism. Thus, in the present work we experimentally examined a fundamental but more limited CO_2 reduction; the key first reduction to formate by a chemically prepared (and different) organo-hydride donor that avoids the participation of proton transfer.

Before proceeding, we provide some perspective on CO_2 reduction via the use of other, non-organic hydrides. Transition metal (TM) hydrides are the most commonly studied hydrides and have proven effective for the reduction of CO_2, and thus merit discussion here. Some efforts have focused on determining the relative hydricity of TM hydrides, the thermodynamic property which quantifies their potency as hydride donors.[12-15] Strong TM hydrides typically involve noble metals, such as $[Ru(tpy)(bpy)H]^+$ and $[Pt(depe)_2H]^+$; typ = 2,2′:6′,2″-terpyridine; bpy = 2,2′-bipyridine; depe = 1,2-bis(diethylphosphino)ethane.[14] Recent advances using non-precious metal species,[7, 16] such as $Co(dmpe)_2H$, have been achieved in the reduction of CO_2 to $HCOO^-$ (formate), but this requires a strong sacrificial base to form the requisite reducing complex *in situ*; dmpe = 1,2-bis(dimethylphosphino)ethane.[7] Beyond the realm of TM-catalyzed processes, only one example of a recycable organo-hydride has been experimentally demonstrated to reduce CO_2 to $HCOO^-$.[8] Yet, even here, the intermediacy of a transition metal center, specifically ruthenium, is required: a dihydropyridine organo-hydride (which ultimately acts as the reductant) forms part of a pbn (2-(pyridin-2-yl)benzo[b][1,5]naphthyridine)) ligand of a $Ru(bpy)_2(pbnH_2)^{2+}$ complex. Moreover, in this system a stoichiometric quantity of a Brønsted base is required to facilitate the transfer of the hydride from the pbn ligand of the Ru complex to CO_2.[17]

While many transition metal-catalyzed and -coupled complexes effectively reduce CO_2 to formate (and beyond), the unfortunate fact remains that the high cost of homogeneous noble metal catalysts effectively hampers the development of economical processes catalyzed by these complexes for the production of utilizable fuels from CO_2. Furthermore, the selectivity of metal-based electrocatalysts is often limited because byproducts such as CO and/or H_2 are formed in addition to formate.[18-21] While CO and H_2 are difficult to store and transport, formate (and formic acid) represents a promising energy carrier candidate, due to its low toxicity, easy transportation and straightforward handling.[22-24]

Scheme 1. Reduction of CO_2 to formate anion by benzimidazole-based organo-hydrides.

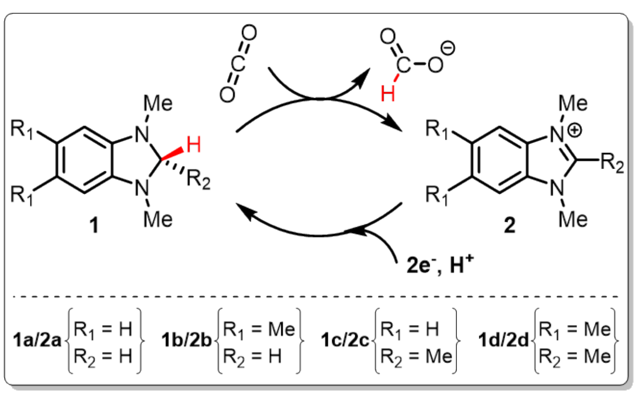

Here we report what is to the best of our knowledge the first reduction of CO_2 to $HCOO^-$ by a metal-free and recyclable organo-hydride derived from benzimidazoles (Scheme 1). Benzimidazoles, direct analogs to imidazole-based cofactors present in 5,10-methenyltetrahydromethanopterin (Hmd) hydrogenase,[25] have been previously identified as promising hydride donors[26-28] due to their characteristic conformation and an anomeric effect.[29] The choice of this hydride donor, the conception of the reduction's mechanism, and results of the reduction were further guided by quantum chemical calculations. An additional noteworthy aspect of the CO_2 reduction illustrated in Scheme 1 is that the reaction proceeds in the absence of biological enzymes,[30] a sacrificial Lewis acid, or a base to activate the substrate or reductant.[31] Specifically, we demonstrate that dihydrobenzimidazole organo-hydrides (1,3-dimethyl-2,3-dihydro-1H-benzimidazole derivatives, species **1a-d** in Scheme 1) are capable of chemically reducing CO_2 to $HCOO^-$ in DMSO solvent. The choice of the solvent used was two-fold: (i) it is a polar solvent that helps stabilize the charged products (benzimidazolium cations and formate), while not possessing acidic protons (like methanol and water) prevents a possible hydrogen evolution reaction from the hydride; (ii) both benzimidazole-hydride and CO_2 are sufficiently soluble in DMSO.

While CO_2 reduction by metal-free hydrides has been previously achieved with organoboranes and organosilanes,[32-42] the inability to regenerate their active hydride forms has restricted their use to only stoichiometric conditions;[26] notably, significant progress has been made to employ dihydrogen in sustainable CO_2 reduction processes catalyzed by Lewis acid and base pairs.[43-45] In our attempt to identify a catalytic CO_2 reduction system, we have electrochemically transformed benzimidazolium cation (1,3-dimethyl-1H-benzimidazol-3-ium derivative **2c**) to its corresponding organo-hydride **1c** with quantitative yield. Thus, the present system serves as a proof of concept that organo-hydrides are capable of transferring a hydride ion to CO_2 and that the regeneration of the hydride can be achieved electrochemically.

COMPUTATIONAL METHODS

All stationary geometries (reactants, transition states and products) for the systems studied were computed using density functional theory based on the M06 density functional[46] and 6-31+G** basis set.[47] To account for the effect of solvent, the implicit polarized continuum solvation model (CPCM)[48-49] was employed in all calculations to treat the solute-solvent electrostatic interactions in dimethyl sulfoxide (DMSO) solvent. Calculated values for relevant standard reduction potentials and pK_a values were obtained following the previously published procedure.[27] All reported energies were referenced to separated reactants in solution and calculations were performed using the GAUSSIAN 09 or 16 computational software packages.[50] The supporting information (SI) sections 1 and 9 provide a more detailed description of the calculated values.

EXPERIMENTAL SECTION

General methods. Benzimidazole (98%), 5,6-dimethylbenzimidazole (≥99%), 2-methylbenzimidazole (98%), iodomethane (99%), 1,3,5-trimethoxybenzene (≥99%), sodium borohydride (99%), $^{13}CO_2$ (99 atom % ^{13}C, <3 atom % ^{18}O), potassium iodide (≥99%), potassium bromide (≥99%), sodium iodide (≥99%), lithium bromide (≥99%) and potassium hexafluorophosphate (≥99%) were purchased from Sigma-Aldrich and used as received. Potassium nitrate (≥99%), potassium perchlorate (≥99%), and potassium tetrafluoroborate (98%) were purchased from Alfa Aesar and used as received. A $^{12}CO_2$ gas cylinder was purchased from Air Products (Bone Dry, 99.9%). DMSO-d_6 (d, 99.9%), MeCN-d_3 (d, 99.8%) and methanol-d_4 (d, 99.8%) were purchased from Cambridge Isotope Laboratories, Inc. DMF-d_7 (d, 99.5%) was purchased from Sigma-Aldrich. Glass tube reactors were purchased from Ace Glass Incorporated: Tube, 9 ml, 150 psig, 19 mm O.D., 10.2 cm long (part # 8648-62). ^{1}H and ^{13}C NMR spectroscopies were performed in a Bruker Ascend 400 MHz spectrometer at the University of Colorado Boulder NMR facility. Chemical shifts are referenced to the internal solvent resonance (DMSO, 2.50 ppm) and reported as parts-per-million (ppm). ESI-MS analysis was performed with a Synapt G2 HDMS Qtof (Waters) at the University of Colorado Boulder mass spectrometry facility. The generalized synthetic procedures were modified from those already reported in the literature.[28, 51]

General experimental procedure for the synthesis of benzimidazoliums (2). The method we describe here was used to synthesize species **2c** and it generally applies to the synthesis of other benzimidazoliums (**2**). 60 mL of reagent grade methanol (0.83 M) was added to a 250 mL round bottom flask equipped with a magnetic stir bar, followed by the addition of 6.61 g (50.0 mmol, 1.00 equiv) of 2-methylbenzimidazole, 12.5 mL (28.5 g, 200 mmol, 4.00 equiv) of iodomethane, and, finally, 6.91 g (50.0 mmol, 1.00 equiv) of potassium carbonate (K_2CO_3). This suspension was subsequently heated at reflux for 18 hours. After cooling the reaction to room temperature, the solution was reduced in volume to ~30 mL *in vacuo* and the solids were filtered through a filter paper-topped Buchner filter. The filtered solids, which contained both residual K_2CO_3 and the desired product 1,2,3-trimethyl-1H-benzimidazol-3-ium iodide (species **2c**) were added to a 250 mL round bottom flask containing 150 mL of reagent grade MeOH and heated to 60ºC to dissolve most, but not all of the solids. The hot solution was then filtered through a Buchner funnel and the filtrate was collected and placed into a freezer (~ -20°C) for 4 hours. After this time the formed crystals were filtered from the supernatant, washed with additional portions of reagent grade acetone (50 mL, 2x), and dried under vacuum to give 10.9 g (76% yield) of the desired 1,2,3-trimethyl-1H-benzimidazole-3-ium iodide (**2c**) as a white solid which was used in the subsequent reaction with no further purification. ^{1}H NMR (400 MHz, DMSO-d_6) δ 8.03 – 7.94 (m, 2H), 7.68 – 7.59 (m, 2H), 4.00 (s, 6H), 2.87 (s, 3H). ^{13}C NMR (101 MHz, DMSO-d_6) δ 152.25, 131.29, 125.81, 112.69, 31.72, 10.62. HRMS (ESI): $C_{10}H_{13}N_2^+$ calculated at 161.1079; observed at 161.1078. See SI section 4 for characterization of other benzimidazoliums (**2**).

General experimental procedure for the synthesis of dihydrobenzimidazoles (1). The method we describe here was used to synthesize species **1c** and it generally applies to the synthesis of other dihydrobenzimidazoles (**1**). 40 mL of H_2O and 60 mL of reagent grade diethyl ether (1.0:1.5, v:v, 0.10 M total dilution) were added to a 250 mL round bottom flask equipped with a magnetic stir bar. Next, 2.88 g (10.0 mmol, 1.00 equiv) of 1,2,3-trimethyl-1H-benzimidazole-3-ium iodide **(2c)** was added, followed by 1.13 g (30.0 mmol, 3.00 equiv) of sodium borohydride in small portions. This mixture was allowed to react under vigorous stirring for 1 hour at room temperature. After this time, the reaction mixture was placed into a separatory funnel and the organic layer was extracted, then washed with deionized water (50 mL, 2×), and finally washed with brine (50 mL, 1×). The organic solution was dried over $MgSO_4$, filtered, and concentrated under reduced pressure to yield 1.05 g (65% yield) of the title compound (**1c**) as a clear liquid. The product was stored under argon in a ~ -20ºC freezer until later use. We note that species **1c** solidified in the freezer at ~ -20ºC and is stable for months when stored at ~ -20ºC even after repeated exposure to air. ^{1}H NMR (400 MHz, DMSO-d_6) δ 6.59 – 6.50 (m, 2H), 6.42 – 6.33 (m, 2H), 4.00 (q, J = 5.3 Hz, 1H), 2.61 (s, 6H), 1.39 (d, J = 5.3 Hz, 3H). ^{13}C NMR (101 MHz, DMSO-d_6) δ 142.59, 118.68, 105.65, 86.13, 33.52, 18.13. HRMS (ESI): $(C_{10}H_{14}N_2)Li^+$ calculated at 169.1317; observed at 169.1319. See SI section 4 for characterization of other dihydrobenzimidazoles (**1**).

General experimental procedure for the reduction of CO_2 with a representative benzimidazole hydride. 31.5 mg (0.25 mmols, 20.00 equiv) of KBF_4 was added to an oven-dried 9 ml glass tube reactor (as shown in SI section 2, Figure S1; purchased from Ace Glass Incorporated) equipped with a 9.5 × 4.7 mm egg-shaped magnetic stir bar purchased from VWR. This was then diluted with 500 µL of DMSO-d_6 containing 2.0 mg (0.0125 mmol, 1.00 equiv) of species **1c** and 4.2 mg (0.025 mmol, 2.00 equiv) of 1,3,5-trimethoxybenzene (as the internal standard) using a calibrated pipette. The tube was then sealed and degassed under vacuum while under sonication for a total of 5 minutes. After degassing, the valve connected to the vacuum was closed and $^{12}CO_2$ at 20 psig (or $^{13}CO_2$ at ~20 psig) was then introduced to the reaction vessel. The reaction mixture temperature was maintained at 50°C in an oil bath for 18 hours while stirring at 800 rpm. After this time, species **1c** was fully consumed and an additional 200 µL of DMSO-d_6 (in some cases methanol-d_4) was added to improve the solubility of the solution. The reaction solution was then analyzed by ^{1}H NMR spectroscopy (and in some cases ^{13}C NMR spectroscopy).

Cyclic voltammetry and digital simulations. Cyclic and linear sweep voltammetries were performed using a BASi epsilon potentiostat in a VC-2 voltammetry cell (Bioanalytical Systems) using a glassy carbon (3 mm diameter, MF-2012, Bioanalytical Systems) or tin (3 mm diameter, custom made, Bioanalytical Systems) working electrode, a nonaqueous Ag/Ag^+ reference electrode (MF-2062, Bioanalytical Systems) and a platinum wire (MW-4130, Bioanalytical Systems) as a counter electrode. The spectroscopic grade solvent DMSO and the electrolyte tetrabutylammonium perchlorate (TBAP) were purchased from Sigma Aldrich and used as received. Electrochemical potentials were converted to NHE by adding 0.569 V to the experimental potentials.[52] For cyclic voltammetry (CV) measurements, the iodide salt of **2c** was converted to perchlorate using a previously published procedure.[53] The CV was simulated using DigiSim simulation software with the following parameters: (i) Electrode area: 0.07 cm^2, planar electrode geometry, scan rate: 100 mV/s, resistance uncompensated; (ii) Semi-infinite diffusion model, diffusion constants for all species calculated using a Stokes radius obtained from optimized structures ($D = 2.8 \cdot 10^{-6}$ cm^2/s), initial concentration of **2c**: 1 mM; (iii) Mechanism: $A + e^- \rightarrow B$ ($E^0 = -1.96$ V, Table S2); B = C (K and k_f for this process was varied, see SI); $C + e^- \rightarrow D$ ($E^0 = 0.30$ V, Table S2); (iv) Electron transfer kinetics were simulated using the Butler-Volmer model with the parameters: α/λ=0.5 eV, k_S=10 cm/s. For details, see SI section 10.

Controlled potential electrolysis. Bulk electrolysis was performed in a glovebox using a BASi Epsilon^{TM} potentiostat in a VC-2 voltammetry cell (Bioanalytical Systems), with a carbon fiber paper working electrode (Freudenberg H23, Fuel

Cell Store), a nonaqueous Ag/Ag$^+$ reference electrode (MF-2062, Bioanalytical Systems) and a coiled platinum wire in an auxiliary electrode chamber (MW-1033 and MR1196, Bioanalytical Systems) as the counter electrode. The electrolysis was performed in deuterated DMSO-d_6 with 1,3,5-trimethoxybenzene (as the internal standard) while its progress was monitored using ^{1}H-NMR spectroscopy. For details, see SI section 11.

RESULTS AND DISCUSSION

Benzimidazole organo-hydrides for CO_2 reduction to formate. A number of previous studies have suggested that benzimidazole-based organo-hydrides are potentially strong hydride donors.[4, 14, 26-28, 54] We used density functional theory (DFT) to calculate the thermochemical properties of CO_2 reduction to $HCOO^-$ by four different benzimidazole-based organo-hydrides (**1a-d**) in order to determine if such hydrides are competent for this reduction. Table 1 shows that species **1a** (the simplest dihydrobenzimidazole considered, where R_1 = H and R_2 = H) is predicted to reduce CO_2 to $HCOO^-$ with a calculated reaction free energy of ΔG^0_{rxn} = 4.2 kcal/mol, while regenerating species **2a**. Species **1b**, where R_1 = Me and R_2 = H, is predicted to be a stronger hydride donor relative to our base case **1a**; ΔG^0_{rxn} is now lowered to 2.0 kcal/mol. We calculate that substitution of Me at R_2 further improves the hydride donation strength such that ΔG^0_{rxn}= 0.7 kcal/mol for **1c**. Finally, **1d** with Me substituted at both R_1 and R_2 is predicted to be the strongest hydride donor reducing CO_2 to $HCOO^-$ with ΔG^0_{rxn}= -1.7 kcal/mol.

Table 1: Predicted thermochemical properties of CO_2 reduction by reductants 1a-d with their corresponding experimental formate yields.

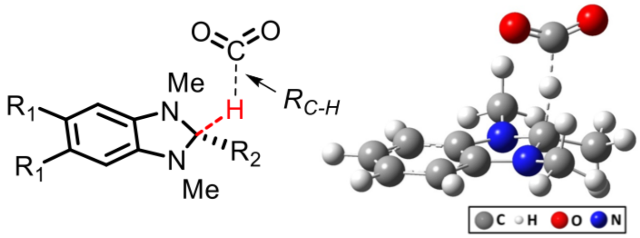

Hydride donor	Formate yield (%)[a]	$\Delta G^{\ddagger}_{HT}$ (298 K) (kcal/mol)[d]	ΔG^0_{rxn} (298 K) (kcal/mol)[d]	$R_{C\text{-}H}$ (Å)[e]
1a	5[b]	23.1	4.2	1.37
1b	4[b]	22.1	2.0	1.39
1c	59[b] (66)[c]	20.6	0.7	1.38
1d	51[c]	21.1	-1.7	1.39

[a]Experimental yields determined by ^{1}H-NMR spectroscopy using 0.05 M of 1,3,5-trimethoxybenzene as an internal standard and species **1** as the limiting reagent. [b]Reaction conditions: 0.50 ml DMSO-d_6, [hydride donor] = 0.10 M, [KBr] = 0.50 M, P_{CO2} = 30 psig, T = 50°C and t = 24 h (except t = 11 h for **1c**). [c]Reaction conditions: 0.50 ml DMSO-d_6, [hydride donor] = 0.025 M, [KBF_4] = 1.00 M, P_{CO2} = 20 psig, T = 50°C and t = 18 h. [d]Theoretical activation free energies ($\Delta G^{\ddagger}_{HT}$) and reaction free energies (ΔG^0_{rxn}) at standard conditions of 298 K and 1 atm, computed at the rM06/6-31+G(d,p) level of theory in implicitly described (CPCM) DMSO solvent. [e]Calculated bond distance between the transferring hydride (H^-) and the carbon (C) of CO_2 at the transition state. The ball-and-stick model shows the computed TS structure for reductant **1c**.

Our initial experimental results, reported in Table 1, are consistent with these calculations (except for the case of **1d**). The hydride donor **1c** produced the correspondingly highest yield of $HCOO^-$ (59%) relative to weaker donors **1a** and **1b** (5% and 4%, respectively). These reactions were performed under mild conditions (T= 50°C and P_{CO2}= 30 psig) in DMSO-d_6 for 24 hours or less (11 hours for **1c**); the addition of salts such as KBr was empirically discovered to significantly increase the yield of formate (*vide infra*). Modifying the reaction conditions resulted in an increase in $HCOO^-$ yield by **1c** to 66%, while **1d** produced a lower yield of 51% despite it being predicted to be a stronger hydride donor. Both **1c** and **1d** suffer from parasitic side reactions in DMSO that prevents their quantitative $HCOO^-$ yield;[55] **1d** is a stronger hydride donor and thus suffered more from non-productive side reactions, thus explaining its lower formate yield relative to **1c** (*vide infra*).

The presumed formation of formate in our reaction was confirmed by its detection under synthetically relevant conditions via both ^{1}H-NMR spectroscopy and electrospray ionization mass spectrometry (ESI-MS). The ^{1}H-NMR spectra obtained after completion of the reaction exhibited a peak at 8.46 ppm, which was confirmed to be formate by comparison to the authentic sample (see SI section 5). To further confirm formate's presence, ESI-MS in negative ion mode was employed. The formate anion was observed to complex with the added salts: for example, in SI section 6, we discuss our detection of the presence of the KBr·$HCOO^-$ complex in the correct isotopic ratios with m/z = 162.9, 164.9, and 166.9. Thus, these two analytical methods confirm the presence of formate in our product solution.

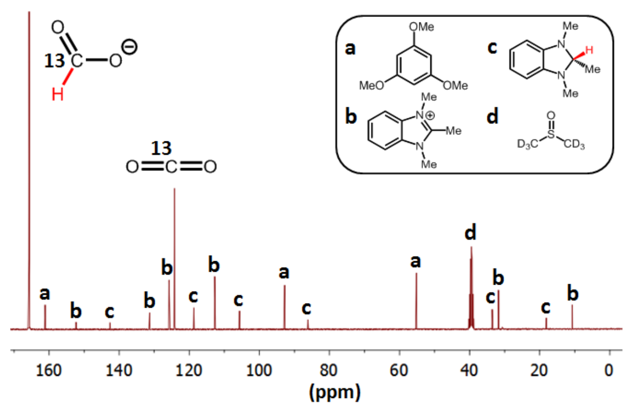

Figure 1. ^{13}C-NMR spectra of species **1c** reacted with $^{13}CO_2$ in DMSO-d_6. Reaction conditions: [**1c**] = 0.10 M, [KBr] = 0.20 M, P_{CO2} = ~20 psig, T = 50°C and t = 16 h. 0.05 M 1,3,5-trimethoxybenzene was introduced as an internal standard. ^{13}C-formate appeared at 165.70 ppm; dissolved $^{13}CO_2$ appeared at 124.18 ppm.[56]

To further validate our proposed mechanism of reduction, we conducted experiments with isotopically enriched $^{13}CO_2$ gas (99 atom % ^{13}C). Figure 1 confirms the presence of $H^{13}COO^-$ (appearing at 165.70 ppm; see SI section 7 for comparison to the authentic sample) in the product solution after

$^{13}CO_2$ reacted with hydride species **1c**. The significant enhancement of $H^{13}COO^-$'s ^{13}C-NMR signal relative to other species in the solution (peaks a-d) is apparent in Figure 1. In addition, in SI section 7, we show that the ^{13}C nuclear spin splits the ^{1}H-NMR peak of $H^{13}COO^-$ into a doublet (at 8.27 and 8.72 ppm), further corroborating the presence of isotopically enriched $H^{13}COO^-$. These results demonstrate that the formate anion detected in the reaction mixture is derived from the chemical reduction of the carbon dioxide introduced to our solution.

Effect of salts and solvents. During the course of these studies, we empirically discovered that the addition of various salts to the reaction mixture greatly enhances the observed formation of the formate anion. A similar salt effect was reported for a photochemically driven system involving the reduction of CO_2 by pyridine[57] and in the catalytic formation of acrylate from ethene and CO_2.[58] Table 2 indicates that in the absence of salts, the $HCOO^-$ yield by **1c** was nearly undetectable (5%, entry 1). Alternatively, under various reaction conditions, the presence of salts (e.g. KBr, KI, LiBr and NaI) resulted in markedly higher yields of the reduced product (25-59%, entries 2-7). Of these salts, KBr produced the highest formate yield (59%, entry 3) relative to other salts under identical conditions.

We propose that adding salts creates a more polar environment that stabilizes ionic products (species **2c** and $HCOO^-$) by increasing the ionic strength of the solution, and thus biases the equilibrium towards the formation of ionic products. In fact, our calculations of a model including the salt KBr suggest that the salt effect significantly improves the thermodynamics of the hydride transfer reaction from $\Delta G^0_{rxn} = 0.7$ kcal/mol to $\Delta G^0_{rxn} = -7.1$ kcal/mol.

Table 2. Reaction of species 1c or 1d with CO_2 under various experimental conditions.

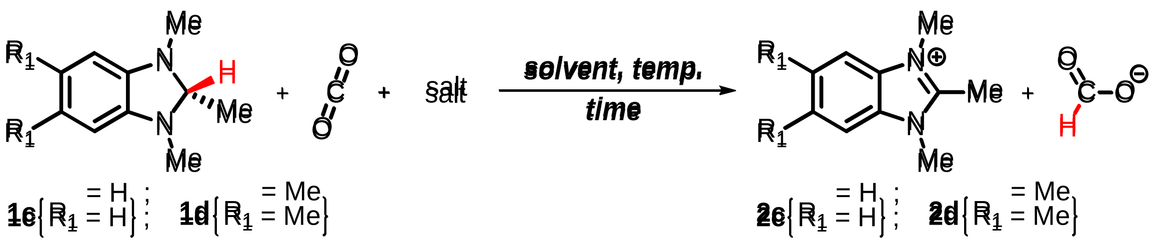

Entry[a]	Hydride donor	[Hydride donor] (M)	Salt	[Salt] (M)	CO_2 (psig)[b]	Time (h)	Consumption of **1** (%)[c]	Formation of **2** (%)[c]	Recovery of **2** (%)	Formate Yield (%)[c,d]
1	1c	0.100	-	-	30	24	69	69	100	5
2	1c	0.100	KBr	0.20	30	11	86	86	100	40
3	1c	0.100	KBr	0.50	30	11	92	91	99	59[e]
4	1c	0.100	KI	0.50	30	11	82	82	100	40[e]
5	1c	0.100	LiBr	0.50	30	11	95	94	99	36[e]
6	1c	0.100	NaI	0.50	30	11	87	86	99	25[e]
7[f]	1c	0.100	KBr	0.50	30	24	79	77	97	33
8	1c	0.050	KBF_4	0.50	20	18	97	96	99	57
9	1c	0.025	KBF_4	0.50	20	18	100	99	99	61
10	1c	0.025	KBF_4	1.00[g]	20	18	100	100	100	66
11	1c	0.025	$KClO_4$	0.50	20	18	100	100	100	35
12	1c	0.025	KNO_3	0.50	20	18	100	100	100	49
13	1c	0.025	KPF_6	0.50	20	18	100	100	100	17
14	1d	0.025	KBF_4	1.00[g]	20	18	100	100	100	51
15	1d	0.025	KNO_3	1.00	20	18	100	99	99	53

[a]All reactions were conducted in 0.50 ml of DMSO-d_6 solvent at 50°C, unless otherwise specified; the solution appeared slightly cloudy after reactions were completed, 0.20 ml of methanol-d_4 (entries 1-7) or 0.20 ml of DMSO-d_6 (entries 8-15) were added to the solution to improve solubility prior to acquiring NMR spectra. [b]Pressure of introduced CO_2 in psig. [c]Determined from ^{1}H-NMR spectroscopy using 0.05 M of 1,3,5-trimethoxybenzene as an internal standard. [d]Yield based on species **1** as the limiting reagent. [e]Formate yield was determined from the average of three runs, with reproducibility of ±5%. [f]Reaction at 25°C. [g]Salt not fully soluble.

Although we first performed the CO_2 reductions at slightly elevated temperatures (50°C, entries 1-6), we anticipated that, in view of the predicted relatively low free energy activation barrier $\Delta G^{\ddagger}_{HT}$ (298 K) = 20.6 kcal/mol in Table 1, species **1c** could still be capable of reducing CO_2 to $HCOO^-$ at room temperature, T = 25°C. Indeed, species **1c** was found to be effective as a reductant under ambient conditions, although lower yield of formate was obtained (33%, t = 24 h, entry 7), presumably due to the slower reaction rate. We also examined this reduction in several solvents: methanol-d_4, MeCN-d_3, and

DMF-d_7 yielded essentially no formate. Mixed solvents comprising of DMSO-d_6 with methanol-d_4, MeCN-d_3, or DMF-d_7 in 1:1 ratios by volume produced lower formate yields relative to pure DMSO-d_6 (see SI section 8, Table S1). D_2O was not examined as a solvent due to **1c**'s poor solubility and tendency to react with water to form H_2, as mentioned below. We propose that the observed reduced activity in methanol-d_4, MeCN-d_3 and DMF-d_7 solvents is caused by their lower polarities (their polarity index values are 5.1, 5.8, and 6.4, respectively, compared to 7.2 for DMSO-d_6).[59] Just as was argued above in connection with the salt effect on the reaction, the lower solvent polarity is presumed to disfavor ionic product formation leading to reduced product yields.

Reaction optimization and side reactions. In an effort to further increase formate yield (beyond the 59% yield of entry 3 of Table 2), we varied **1c**'s concentration, types of potassium salts, salt concentration, CO_2 pressure, and length of reaction time (Table 2, entries 8-13; also see SI Table S1). We found that by both lowering [**1c**] from 0.100 M to 0.025 M and increasing the reaction time from 11 h to 18 h, we were able to fully consume hydride donor **1c** to quantitatively form **2c**; however, not all **1c** was consumed to form the desired formate product as some reacted in parasitic side reactions (*vide infra*). From the results reported in Table 2 and Table S1 we also determined that a CO_2 pressure of 20 psig produced a slight improvement over 30 psig while a higher CO_2 pressure of 40 psig yielded poorer results (*vide infra*). At the reaction conditions of [**1c**] = 0.025 M, P_{CO2} = 20 psig, t = 18 h and 0.50 M of KBF_4, formate yield improved to 61% (entry 9). Notably, KBF_4 gave a higher formate yield than the potassium salts $KClO_4$, KNO_3 and KPF_6 under identical conditions (entries 11-13). When [KBF_4] was increased to 1.00 M or 40 equiv. relative to **1c**, formate yield was further increased to 66% (entry 10).

Under these optimized conditions, we tested the performance of **1d** (see SI section 3 for the synthetic procedure). **1d** was computationally predicted to be a slightly stronger hydride donor than **1c,** due to the moderate electron-donating ability of the methyl groups at the 5 and 6 positions of the benzimidazole. As reported in Table 1, **1d** was predicted to reduce CO_2 to formate with the following properties: $\Delta G^{\ddagger}_{HT}$ = 21.1 kcal/mol, ΔG^{0}_{rxn} = -1.7 kcal/mol, and $R_{C\text{-}H}$ = 1.39 Å. However, despite being predicted as a stronger hydride donor, **1d** produced formate yields of only 51% (1.00 M KBF_4, entry 14) and 53% (1.00 M KNO_3, entry 15), lower than the 66% (entry 10) produced by **1c** (while **1d** was fully reacted to generate **2d**). As we describe next, the hydrides of **1c** and **1d** participated in parasitic reactions that limit their formate yields.

We have identified two potential channels for the non-productive consumption of hydride donors **1c** and **1d**. First, we anticipate that the hydride can react with trace water in DMSO (present due to its hygroscopic nature) to form H_2 and hydroxide OH^-.[60] Second, the hydride could also non-productively react with DMSO to form dimethyl sulfide[55] and OH^-. The OH^- generated from these two sources likely reacts with excess CO_2 in the solution to form bicarbonate (HCO_3^-); this anion may then complex with potassium cations present in the solution to form the less soluble $KHCO_3$ salt. Indeed, this may well explain the observed cloudiness of the solution after completion of the reaction. Furthermore, we observed that formate yield by **1c** was significantly lowered to 12% at a higher CO_2 pressure of 40 psig, as reported in Table S1. Following an argument similar to that above, we hypothesize that the larger excess of CO_2 increased OH^- consumption, which in turn increased the parasitic consumption of **1c** and **1d**, thereby resulting in lower formate yields. Given that **1d** is a stronger hydride donor, the parasitic consumption of its hydride was presumably more severe, thus producing a lower formate yield than **1c**. Future design of the hydrides will focus on improving the kinetics of CO_2 reduction, while preventing the parasitic loss of the hydrides.[61]

Connections to dihydropyridine. Interestingly, the benzimidazole-based hydride systems studied here closely resemble our previously studied dihydropyridines, whose NADPH analogue is used as a recyclable hydride in natural photosynthetic CO_2 fixation.[9-10] Although, as explained in the Introduction, the present study is deliberately restricted compared to ref. 10 --- with a focus on examining the fundamental concept of CO_2 reduction by hydride transfer --- it is instructive to note key points of commonality.

Perhaps the most important among several key features in common between these two chemistries is a hydride bound to a carbon that neighbors a N atom of a ring that becomes aromatic upon transfer of the hydride; this provides an analogous source for the driving force for hydride transfer. The underlying dearomatization-aromatization cycle that creates the thermodynamic driving force for CO_2 reduction was previously uncovered in the pyridine system.[62,10] Similarly, because the aromatic species **2** is dearomatized upon its reduction to compound **1**, the proclivity of this latter species to re-aromatize drives it to transfer H^- to CO_2 to form the formate product while recovering the aromatic species **2**. While ref. 10 includes the next protonation step of formate to produce formic acid that is not addressed here, the experimental results we report confirm the reduction of CO_2 by **1**, and support the proposed theoretical homogeneous hydride transfer mechanism for the reduction of CO_2 to methanol.[10-11] For an extended discussion and references, see ref. 9.

Electrochemical regeneration. As determined by ^{1}H-NMR spectroscopy, **1** was consumed to quantitatively recover the oxidized and aromatic species **2** (Table 2), thereby establishing its potential to function as a recyclable organo-hydride. Here, we examine the possibility of regenerating **1c** from **2c** electrochemically to achieve catalytic CO_2 reduction. Generally, the recovery of **1** from the oxidized species **2** requires a net transfer of two electrons and a proton. Three possible pathways for electrochemical regeneration are represented in Scheme 2. The first pathway (pathway i) involving the protonation of **2c** followed by two successive electron transfers (ETs) has been discarded because of the inability to protonate the benzimidazolium species **2c** due to its high free energy cost. In contrast, the other two pathways in Scheme 2 (ii and iii) include an initial ET which leads to the formation of a neutral radical **2c$^\bullet$**. The fate of **2c$^\bullet$** depends on experimental conditions (e.g. applied electrochemical potentials and the presence of acids). Even though the second ET is calculated to be feasible at applied potentials (pathway ii), a rapid dimerization of **2c$^\bullet$** impedes further recovery of the dihydrobenzimidazole hydride species **1c**.[63] Finally, in the presence of a proton source, the facile protonation of the radical **2c$^\bullet$** enables a subsequent exergonic electron transfer that leads to formation of the hydride **1c** (pathway iii).

Inspired by the favorable calculated thermodynamic parameters for the electrochemical regeneration, we performed cyclic voltammetry (CV) experiments in the presence (pathway iii) and absence (pathway ii) of acids. Specifically, Figure 2a shows CVs of **2c** obtained with different scanning directions in the presence and absence of phenol acting as a weak proton donor. In both cases, the irreversible reduction peaks appear at −1.88 V vs. NHE, which is consistent with the calculated one-electron reduction potential for **2c**/**2c**$^{\bullet}$ conversion (see SI section 9, Table S2). Interestingly, the current intensity doubled in the presence of phenol indicating a possible proton-coupled two-electron transfer process, as represented in pathway iii (Scheme 2). Similar behavior was observed when stronger acids (acetic, chloroacetic and tetrafluoroboronic acids) were employed.

Scheme 2. Sequential regeneration pathways for electrochemical conversion of species 2c to hydride-active species 1c.

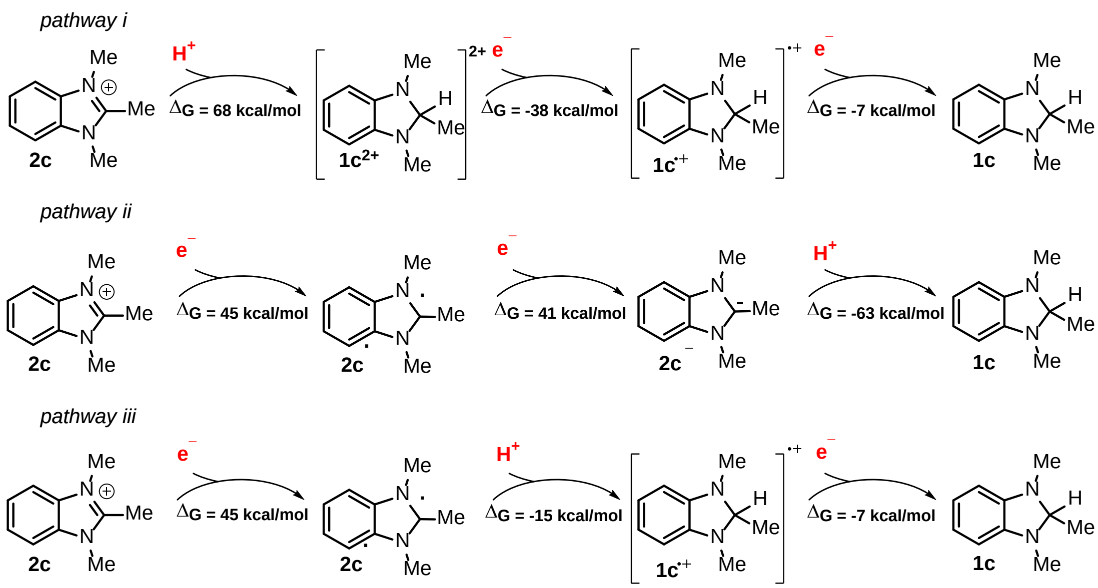

Indeed, scanning to positive potentials from these reduction peaks (scan direction: −2.3 V to +0.75 V) resulted in the appearance of a peak at ~ +0.3 V vs. NHE only in the presence of the acid. The peak matches well with the calculated oxidation peak of species **1c** (+0.30 V vs. NHE, Table S2). To confirm this regeneration, we performed the electrochemical oxidation of an authentic sample **1c**; this indeed exhibited an oxidation potential at +0.36 V vs. NHE supporting the electrochemical regeneration of **1c** from **2c** (Figure 2a, inset).

To evaluate the efficiency of electrochemical regeneration of **1c**, the experimental CVs were compared with the simulation, which was computed assuming that **2c** undergoes a proton-coupled two-electron reduction process to form **1c** (Figure 2b). An excellent match was obtained between the experimental and simulated voltammograms, indicating a quantitative conversion of **2c** to **1c** and that no side reactions (e.g. dimerization) occur.

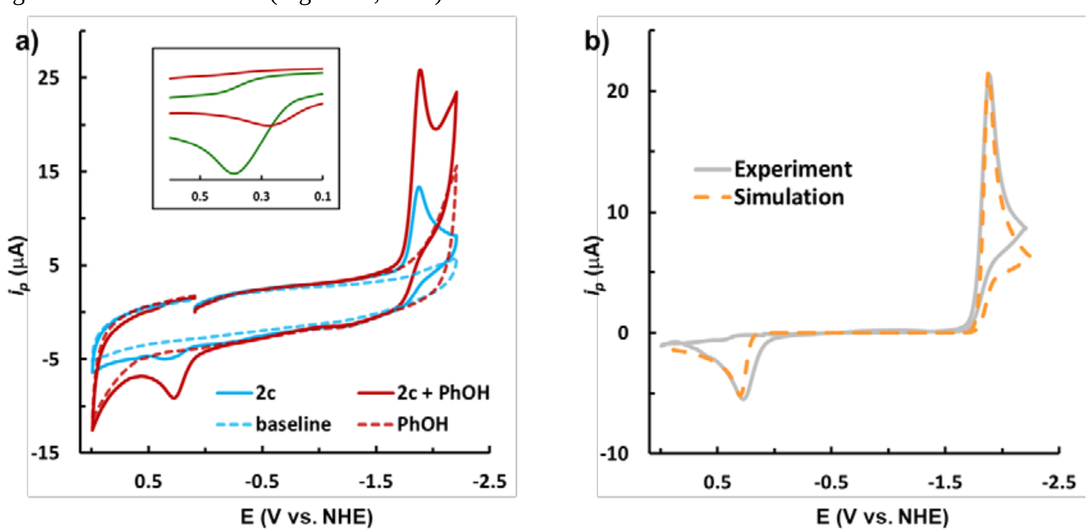

Figure 2. Electrochemical regeneration of **1c** from **2c**. (a) Cyclic voltammograms at scan rates of 100 mV/s of 1 mM **2c** in DMSO with (maroon solid) and without (blue solid) 100 eq. of phenol, baseline scan (blue dashed line) and a scan of a 100 mM solution of phenol in DMSO (maroon dashed line). Scan directions: +0.1 V → –2.3 V → +0.75 V → +0.1 V. Inset: the oxidation of authentic 1 mM solution of **1c** (green); (b) Experimental (baseline subtracted, gray) and simulated (orange dashed) CVs of 1 mM solution of **2c** in the presence of phenol at a scan rate of 100 mV/s. Simulation parameters are described in the SI section 10, with K(PT) = 100 and k_f(PT) = 10^4 s^{-1} giving the closest match to experimental values.

To further confirm and quantify the electrochemical conversion of **2c** to **1c**, we performed a controlled potential electrolysis experiment using a carbon fiber paper working electrode in DMSO-d_6 and an excess of phenol. The electrolysis progress was monitored via ^{1}H-NMR spectroscopy, with 1,3,5-trimethoxybenzene as an internal standard. Over the course of 4 h, **2c** was quantitatively transformed to hydride **1c** (Figure 3) at an applied potential of E_{app} = –1.91 V (vs. NHE). Specifically, after electrolysis, the ^{1}H-NMR spectra of the resulting product matched the authentic sample of **1c** and the integration values (relative to 1,3,5-trimethoxybenzene at ~6.1 ppm) of the aromatic hydrogens were identical (0.56 in Figure 3a and 0.55 in Figure 3b). The full conversion required a slight excess of supplied charge due to the competing proton reduction (Figure 2a). This experiment rules out the possibility that **2c** is involved in any side reactions (e.g. dimerization of the forming radical) in the course of electrolysis under the given experimental conditions, which has often prevented the regeneration of previously studied NADH-analogs.[64-68]

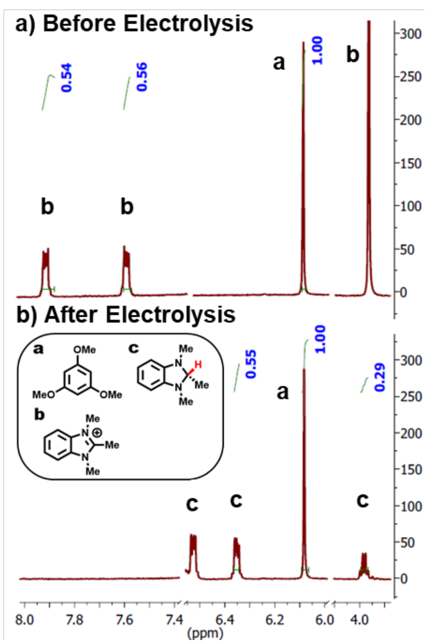

Figure 3. ^{1}H-NMR spectra of catholyte DMSO-d_6 solution of 1 mM **2c** in the presence of 150 equiv of phenol and 1,3,5-trimethoxybenzene as an internal reference, before (a) and after (b) bulk electrolysis on carbon fiber paper as the working electrode at E_{app} = –1.91 V vs. NHE. For clarity, the NMR signals of the excess phenol in the aromatic region were omitted; see SI section 11 for the full spectra.

We note that the relatively slow hydride transfer kinetics (e.g. over hours, see Table 2) impedes the exploitation of the current system for electrocatalytic CO_2 reduction, as we attempted by electrochemical experiments on two different electrodes (glassy carbon and tin) in the presence of CO_2 (see SI section 12 for additional details). We suggest that the hydride transfer kinetics can be improved by tuning the thermodynamic hydricity of benzimidazole-based hydrides.[26-28] In any event, the combined reduction of CO_2 to formate and complete electrochemical recovery of the active hydride form demonstrated here indicate that improving the kinetic properties of the current system could plausibly result in the development of metal-free catalytic systems for solar energy to fuels applications.

CONCLUSIONS

In conclusion, we have demonstrated the unprecedented use of metal-free and recyclable benzimidazole-based organo-hydrides (**1**) for the chemical reduction of CO_2 to formate, a reaction driven by the dearomatization-aromatization[9,10] of the dihydrobenzimidazole/benzimidazolium (**1**/**2**) redox couple. We further established the quantitative regeneration of **1** from **2** via controlled potential electrolysis as proof of concept for conceivable electrocatalytic CO_2 reduction with **1**/**2** redox couple.

This work demonstrates an accessible CO_2 reduction to formate by organo-hydrides, even in the absence of metal-centers. The present results suggest the possibility of completely metal-free hydride sources as alternatives to noble metal-based hydride donors to reduce CO_2 efficiently to usable fuels in a catalytic fashion. This opens the door to future development of related organic species that are reduced to reactive hydrides electrochemically, photochemically or photoelectrochemically powered by renewable energy. In a more extended arena, we hope that the present work will inspire future research to incorporate an appropriate proton source into our proposed catalytic cycle to effect the reduction of CO_2 directly to methanol.

ASSOCIATED CONTENT

Supporting Information. Computational methods, experimental setup for CO_2 reduction, synthesis of **1d** and **2d**, experimental characterization of compounds, ^{1}H NMR for formate detection, ESI-MS for formate detection, ^{1}H NMR and ^{13}C NMR for $^{13}CO_2$ experiment, additional experimental data, calculated values for electrochemical regeneration, cyclic voltammogram (CV) simulations, controlled potential electrolysis (CPE), attempted electrocatalytic CO_2 reduction, and coordinates of calculated molecular structures This material is available free of charge via the Internet at http://pubs.acs.org.

AUTHOR INFORMATION

Corresponding Author

*Charles B. Musgrave (charles.musgrave@colorado.edu)
*Chern-Hooi Lim (chernhooi.lim@colorado.edu)

ACKNOWLEDGMENT

This work is supported in part by NSF grants CHE-1214131 (CBM and CHL), CHE-1112564 (JTH), the ACS PRF grant 54436-ND4 (KDG) and a postdoctoral fellowship from the Arnold and Mabel

Beckman Foundation (BTW). CHL is grateful for an NIH F32 Postdoctoral Fellowship (F32GM122392). We gratefully acknowledge use of XSEDE supercomputing resources (NSF ACI-1053575), Ohio Supercomputer Center PCS0201-5 (KDG) and the Janus supercomputer, which is supported by NSF (CNS-0821794) and the University of Colorado Boulder. We greatly appreciate the use of the laboratory facilities of Chris Bowman at the University of Colorado Boulder. We also thank CU Crowdfunding for financial support, especially the following donors: Lim Kee Moi, Lim Lynn Hwee, Cho Teng Kit and Foo Mei Khoon. We thank Marija R. Zoric for her guidance and assistance with the controlled potential electrolysis experiments.

REFERENCES

1. Appel, A. M.; Bercaw, J. E.; Bocarsly, A. B.; Dobbek, H.; DuBois, D. L.; Dupuis, M.; Ferry, J. G.; Fujita, E.; Hille, R.; Kenis, P. J. A.; Kerfeld, C. A.; Morris, R. H.; Peden, C. H. F.; Portis, A. R.; Ragsdale, S. W.; Rauchfuss, T. B.; Reek, J. N. H.; Seefeldt, L. C.; Thauer, R. K.; Waldrop, G. L., *Chem. Rev.* **2013,** *113*, 6621.
2. Lewis, N. S.; Nocera, D. G., *Proc. Natl. Acad. Sci. U.S.A.* **2006,** *103*, 15729.
3. Deno, N. C.; Peterson, H. J.; Saines, G. S., *Chem. Rev.* **1960,** *60*, 7.
4. Horn, M.; Schappele, L. H.; Lang-Wittkowski, G.; Mayr, H.; Ofial, A. R., *Chem. - Eur. J.* **2013,** *19*, 249.
5. Richter, D.; Mayr, H., *Angew. Chem. Int. Ed.* **2009,** *48*, 1958.
6. Moret, S.; Dyson, P. J.; Laurenczy, G., *Nat. Commun.* **2014,** *5*.
7. Jeletic, M. S.; Mock, M. T.; Appel, A. M.; Linehan, J. C., *J. Am. Chem. Soc.* **2013,** *135*, 11533.
8. Ohtsu, H.; Tanaka, K., *Angew. Chem. Int. Ed.* **2012,** *51*, 9792.
9. Lim, C.-H.; Holder, A. M.; Hynes, J. T.; Musgrave, C. B., *J. Phys. Chem. Lett.* **2015**, 5078.
10. Lim, C.-H.; Holder, A. M.; Hynes, J. T.; Musgrave, C. B., *J. Am. Chem. Soc.* **2014,** *136*, 16081.
11. Lim, C.-H.; Holder, A. M.; Hynes, J. T.; Musgrave, C. B., *J. Phys. Chem. B* **2017,** *121*, 4158.
12. Huang, K.-W.; Han, J. H.; Musgrave, C. B.; Fujita, E., *Organometallics* **2007,** *26*, 508.
13. Muckerman, J. T.; Achord, P.; Creutz, C.; Polyansky, D. E.; Fujita, E., *Proc. Natl. Acad. Sci. U.S.A.* **2012,** *109*, 15657.
14. Matsubara, Y.; Fujita, E.; Doherty, M. D.; Muckerman, J. T.; Creutz, C., *J. Am. Chem. Soc.* **2012,** *134*, 15743.
15. DuBois, D. L.; Berning, D. E., *Appl. Organomet. Chem.* **2000,** *14*, 860.
16. Taheri, A.; Thompson, E. J.; Fettinger, J. C.; Berben, L. A., *ACS Catal.* **2015**, *5*, 7140.
17. Ohtsu, H.; Tsuge, K.; Tanaka, K., *J. Photochem. Photobiol. A* **2015,** *313*, 163.
18. Zhu, D. D.; Liu, J. L.; Qiao, S. Z. *Adv. Mater.* **2016,** *28*, 3423.
19. Costentin, C.; Robert, M.; Saveant, J.-M. *Chem. Soc. Rev.* **2013,** *42*, 2423.
20. Qiao, J.; Liu, Y.; Hong, F.; Zhang, J. *Chem. Soc. Rev.* **2014,** *43*, 631.
21. Francke, R.; Schille, B.; Roemelt, M. *Chem. Rev.* **2018,** *118*, 4631.
22. Sordakis, K.; Tang, C.; Vogt, L. K.; Junge, H.; Dyson, P. J.; Beller, M.; Laurenczy, G. *Chem. Rev.* **2018,** *118*, 372.
23. Eppinger, J. r.; Huang, K.-W. *ACS Energy Lett.* **2016,** *2*, 188.
24. Mellmann, D.; Sponholz, P.; Junge, H.; Beller, M. *Chem. Soc. Rev.* **2016,** *45*, 3954.
25. Shima, S.; Pilak, O.; Vogt, S.; Schick, M.; Stagni, M. S.; Meyer-Klaucke, W.; Warkentin, E.; Thauer, R. K.; Ermler, U., *Science* **2008,** *321*, 572.
26. Ilic, S.; Alherz, A.; Musgrave, C. B.; Glusac, K. D., *Chem. Soc. Rev.* **2018,** *47*, 2809.
27. Ilic, S.; Pandey Kadel, U.; Basdogan, Y.; Keith, J. A.; Glusac, K. D., *J. Am. Chem. Soc.* **2018,** *140*, 4569.
28. Zhu, X.-Q.; Zhang, M.-T.; Yu, A.; Wang, C.-H.; Cheng, J.-P., *J. Am. Chem. Soc.* **2008,** *130*, 2501.
29. Brunet, P.; Wuest, J. D., *J. Org. Chem.* **1996,** *61*, 2020.
30. Calvin, M., *Science* **1962,** *135*, 879.
31. Lim, C.-H.; Holder, A. M.; Hynes, J. T.; Musgrave, C. B., *Inorg. Chem.* **2013,** *52*, 10062.
32. Park, S.; Bézier, D.; Brookhart, M. *J. Am. Chem. Soc.* **2012,** *134*, 11404.
33. Ménard, G.; Stephan, D. W. *J. Am. Chem. Soc.* **2010,** *132*, 1796.
34. Lu, Z.; Hausmann, H.; Becker, S.; Wegner, H. A. *J. Am. Chem. Soc.* **2015,** *137*, 5332.
35. Mukherjee, D.; Osseili, H.; Spaniol, T. P.; Okuda, J. *J. Am. Chem. Soc.* **2016,** *138*, 10790.
36. Chen, J.; Falivene, L.; Caporaso, L.; Cavallo, L.; Chen, E. Y.-X. *J. Am. Chem. Soc.* **2016,** *138*, 5321.
37. Matsuo, T.; Kawaguchi, H. *J. Am. Chem. Soc.* **2006,** *128*, 12362.
38. Courtemanche, M.-A.; Légaré, M.-A.; Maron, L.; Fontaine, F. d. r.-G. *J. Am. Chem. Soc.* **2013,** *135*, 9326.
39. Berkefeld, A.; Piers, W. E.; Parvez, M. *J. Am. Chem. Soc.* **2010,** *132*, 10660.
40. Chakraborty, S.; Zhang, J.; Krause, J. A.; Guan, H. *J. Am. Chem. Soc.* **2010,** *132*, 8872.
41. Bontemps, S.; Vendier, L.; Sabo-Etienne, S. *J. Am. Chem. Soc.* **2014,** *136*, 4419.
42. Zimmerman, P. M.; Zhang, Z. Y.; Musgrave, C. B. *Inorg. Chem.* **2010,** *49*, 8724.
43. Courtemanche, M.-A.; Pulis, A. P.; Rochette, É.; Légaré, M.-A.; Stephan, D. W.; Fontaine, F.-G. *Chem. Commun.* **2015,** *51*, 9797.
44. Ye, J.; Johnson, J. K. *ACS Catal.* **2015,** *5*, 6219.
45. Ashley, A. E.; Thompson, A. L.; O'Hare, D. *Angew. Chem. Int. Ed.* **2009,** *48*, 9839.
46. Zhao, Y.; Truhlar, D. G., *Theor. Chem. Acc.* **2008,** *120*, 215.
47. Hariharan, P. C.; Pople, J. A., *Theor. Chem. Acc.* **1973,** *28*, 213.
48. Li, H.; Jensen, J. H., *J. Comput. Chem.* **2004,** *25*, 1449.
49. Li, H.; Pomelli, C. S.; Jensen, J. H., *Theor. Chem. Acc.* **2003,** *109*, 71.
50. Frisch, M. J.; Trucks, G. W.; Schlegel, H. B.; Scuseria, G. E.; Robb, M. A.; Cheeseman, J. R.; Scalmani, G.; Barone, V.; Petersson, G. A.; Nakatsuji, H.; Li, X.; Caricato, M.; Marenich, A. V.; Bloino, J.; Janesko, B. G.; Gomperts, R.; Mennucci, B.; Hratchian, H. P.; Ortiz, J. V.; Izmaylov, A. F.; Sonnenberg, J. L.; Williams; Ding, F.; Lipparini, F.; Egidi, F.; Goings, J.; Peng, B.; Petrone, A.; Henderson, T.; Ranasinghe, D.; Zakrzewski, V. G.; Gao, J.; Rega, N.; Zheng, G.; Liang, W.; Hada, M.; Ehara, M.; Toyota, K.; Fukuda, R.; Hasegawa, J.; Ishida, M.; Nakajima, T.; Honda, Y.; Kitao, O.; Nakai, H.; Vreven, T.; Throssell, K.; Montgomery Jr., J. A.; Peralta, J. E.; Ogliaro, F.; Bearpark, M. J.; Heyd, J. J.; Brothers, E. N.; Kudin, K. N.; Staroverov, V. N.; Keith, T. A.; Kobayashi, R.; Normand, J.; Raghavachari, K.; Rendell, A. P.; Burant, J. C.; Iyengar, S. S.; Tomasi, J.; Cossi, M.; Millam, J. M.; Klene, M.; Adamo, C.; Cammi, R.; Ochterski, J. W.; Martin, R. L.; Morokuma, K.; Farkas, O.; Foresman, J. B.; Fox, D. J. *Gaussian 16 Rev. B.01*, Wallingford, CT, 2016.
51. Roberts, G. M.; Pierce, P. J.; Woo, L. K., *Organometallics* **2013,** *32*, 2033.
52. Pavlishchuk, V. V.; Addison, A. W., *Inorg. Chim. Acta* **2000,** *298*, 97.
53. Lee, I.-S. H.; Jeoung, E. H.; Kreevoy, M. M. *J. Am. Chem. Soc.* **1997,** *119*, 2722.
54. Alherz, A.; Lim, C.-H.; Hynes, J. T.; Musgrave, C. B., *J. Phys. Chem. B* **2018,** *122*, 1278.
55. Wood, P. M. *FEBS Letters* **1981,** *124*, 11-14.
56. O'Leary, M. H.; Jaworski, R. J.; Hartman, F. C., *Proc. Natl. Acad. Sci. U.S.A.* **1979,** *76*, 673.
57. Boston, D. J.; Xu, C.; Armstrong, D. W.; MacDonnell, F. M., *J. Am. Chem. Soc.* **2013,** *135*, 16252.
58. Lejkowski, M. L.; Lindner, R.; Kageyama, T.; Bódizs, G. É.; Plessow, P. N.; Müller, I. B.; Schäfer, A.; Rominger, F.; Hofmann, P.; Futter, C.; Schunk, S. A.; Limbach, M., *Chem. - Eur. J.* **2012,** *18*, 14017.
59. Snyder, L. R., *J. Chromatogr. A* **1974,** *92*, 223.

60. Hecht, S. M.; Adams, B. L.; Kozarich, J. W., *J. Org. Chem.* **1976,** *41*, 2303.
61. Schwarz, D. E.; Cameron, T. M.; Hay, P. J.; Scott, B. L.; Tumas, W.; Thorn, D. L., *Chem. Commun.* **2005,** *0*, 5919.
62. Barton, E. E.; Rampulla, D. M.; Bocarsly, A. B., *J. Am. Chem. Soc.* **2008,** *130*, 6342.
63. de Robillard, G.; Devillers, C. H.; Kunz, D.; Cattey, H. l. n.; Digard, E.; Andrieu, J., *Org. Lett.* **2013,** *15*, 4410.
64. Micheletti Moracci, F.; Liberatore, F.; Carelli, V.; Arnone, A.; Carelli, I.; Cardinali, M. E. *J. Org. Chem.* **1978,** *43*, 3420.
65. Carelli, I.; Cardinali, M. E.; Casini, A.; Arnone, A. *J. Org. Chem.* **1976,** *41*, 3967.
66. Malinski, T.; Elving, P. J. *J. Electrochem. Soc.* **1982,** *129*, 1960.
67. Schmakel, C. O.; Santhanam, K.; Elving, P. J. *J. Am. Chem. Soc.* **1975,** *97*, 5083.
68. Santhanam, K.; Elving, P. J. *J. Am. Chem. Soc.* **1973,** *95*, 5482.